Natural distinction of carbon and nitrogen isotopic niches in common fish species for diverse marine biotopes off the Yellow River estuary and adjacent sea areas

Pei Qu[1,2*], Min Pang[1,2], Fangyuan Qu[1,2], Zhao Li[3], Meng Xiao[4], Zhaohui Zhang[1,2*]

[1]*First Institute of Oceanography, Ministry of Natural Resources of the People's Republic of China, No. 6, Xianxialing Road, Laoshan District, Qingdao City, Shandong Province, China*

[2]*Pilot National Laboratory for Marine Science and Technology (Qingdao), No. 168, Wenhaizhong Road, Jimo District, Qingdao City, Shandong Province, China*

[3]*China National Environmental Monitoring Centre, Chaoyang District, Beijing City, China*

[4]*Qingdao University of Science & Technology, No. 53, Zhengzhou Road, Shibei Distrct, Qingdao City, Shandong Province, China*

**Corresponding author*: *tel:* +86 0532 8896 1621;

e-mail: qupei@fio.org.cn; *zhangzhaohui@fio.org.cn*

Abstract

Stable isotope analysis is a universally recognized and efficient method of indicating trophic relationships that is widely applied in research. However, variations in natural isotopic abundance may lead to inaccuracies due to the effects of complex environmental conditions. This research compared the carbon and nitrogen isotopic niches of fish communities between diverse biotopes around the Yellow River estuary and adjacent sea areas, with the aim of revealing distinctions in stable isotopic niche metrics, trophic positions, and feeding preferences. Stable isotopic niche results indicated that the communities of estuarine habitants were compatible in most study biotopes, and may provide a corridor for energy and material transportation between Laizhou Bay and the open water. Local biocoenosis was embodied in the wider isotopic niche corresponding to frequent environmental changes and abiotic gradients. This implied that they used various food sources to adapt to the fickle environment, including marine-terrestrial boundaries and the estuary. Our analysis of the food source contribution indicated that allochthonous sources were considered major

energy sources in estuarine areas directly affected by Yellow River-diluted water, while autochthonous benthic and pelagic producers dominated carbon input into the food web in Laizhou Bay and the open water. A significant variation in the fish $\delta^{15}N$ characteristic was found within estuarine adjacent regions, so, together with the results from previous studies, we deemed the local high concentration of dissolved inorganic nitrogen as the original trigger of the abnormal $\delta^{15}N$ characteristic in fishes via a transport process along food chains. These results provide a new perspective on the natural distinction of carbon and nitrogen isotopic niches. The detailed data reported here enhance our understanding of variations in fish communities in estuarine ecosystems.

Key words: stable isotopic niche; estuarine offshore biotope; food source; trophic level, fish community

Introduction

Estuarine biotopes display distinct trophic structures of biocoenosis driven by the supply and transformation of multiple energy sources (Underwood, 2010), while flowing waters sustain riverine and marine biodiversity, and make important contributions to global biogeochemical cycles (Palmer et al., 2019). It is widely believed that most adjacent marine ecosystems are strongly connected due to the water transference of organic matter and bioelements (Stasko et al., 2018; Sujitha et al., 2019). Adjacent ecosystems also provide ecological corridors for animal migration (Hastie et al., 2016). Numerous investigations have shown that transference of energy and materials occurs frequently between biotopes influenced by strong coastal physical and biological dynamics (Livernois et al., 2019). This implies the potential connectivity of trophic niches and biocoenosis structures (Palmer et al., 2019). However, there is relatively little research on identifying discrepancies in fish trophic niches caused by diverse marine biotopes around the estuary directly. These related studies are limited to temporal and spatial heterogeneity in food sources (McMahon et al., 2015) and the complexity of marine ecosystems within various biotopes (Christianen et al., 2017; Ramshaw et al., 2017). Investigations comparing the trophic relationships between diverse biotopes in estuarine ecosystems have seldom been performed, and this has hindered our understanding of the energy and material

transporting mechanisms in the food webs.

Stable isotopes record information of marine lives accumulating nutrients over integrated time periods in lifecycles as opposed to a snapshot of food ingestion (Plass-Johnson et al., 2013). They can be used to reconstruct the trophic structures of biocoenoses in marine food webs (Parnell et al., 2010; Boecklen et al., 2011; Fry, 2013). However, as reality is a bit more complicated, mixed models that take isotope values of multiple food sources into account according to user-specified data have been developed and successfully applied to food web studies to solve complex interpretation processes (Jackson et al., 2011; Phillips et al., 2012). Stable isotopic analysis can greatly contribute to research on fish community connectivity in marine ecosystems on account of isotopic signatures corresponding to estuarine biotopes (Selleslagh et al., 2015). As the trophic relationship can be concisely expounded using stable isotope analysis together with advisable models, such as SIBER (Stable Isotope Bayesian Ellipses in R, Jackson et al., 2011) and IsoSource (Layman et al., 2012), a comparison of trophic relationships of biocoenoses between diverse biotopes, including variations in trophic structures, can be further indicated.

The Yellow River is the second longest river in China and its input routes have changed over time, leading to complicated biotopes in the estuary (Xu et al., 2013). There is a strong interaction between ocean and land as with many large river estuaries, and the research value is significant in terms of the diverse marine food webs within the Yellow River estuary. However, to date, few studies have compared the trophic relationships between diverse biotopes in Yellow River estuarine ecosystems. This shortage of information hinders our understanding of the energy and materials transportation mechanism in local food webs and impedes the restoration and conservation process in estuarine Marine Protected Areas (MPAs).

This research aimed to compare the isotopic niches of fish communities between diverse biotopes in the Yellow River estuary with the main expectation of revealing distinctions in stable isotopic niche metrics, trophic positions, and feeding preferences. These results provide new perspectives on trophic relationships, and they provide detailed data that can enhance our understanding of the variations in fish communities in estuarine ecosystems, with important implications for fishery conservation and the restoration of estuarine MPAs.

Method

Research area and sampling methods

Two sampling cruises were launched in September 2017 and September 2018. Study areas were the coastal sea located from 118.5°E to 119.5°E and 37.0°N to 38.4°N around the Yellow River estuary (Figure 1). The location included five MPAs: Yellow River Estuary MPA, Lijin MPA, Hekou MPA, Laizhou MPA, and Guangrao MPA. MPAs are considered ideal experimental systems in which to obtain environmental background values in areas that restrict human activities. The inherent variety of fish communities in a stable isotopic niche caused by a diverse marine biotope can be compared with different biotopes that exclude direct human exploitation.

Selection of survey biotopes mainly considered the diversity between typical estuarine and gulf ecosystems, as well as subtidal zones and deeper water. Five biotopes (Figure 1) with unique individual characteristics were selected. All five biotopes were separated by the Yellow River estuary and differentiated by intertidal and subtidal zones, and represented environment characteristic data, such as salinity around the Yellow River estuary, which were synthetically used to distinguish the influencing scope of diluted water from the river. Each of these five biotopes had discriminative marine ecosystem characteristics. Biotope-H, located at the intertidal and subtidal zone of the recent Yellow River estuary, was directly affected by the abundant diluted water from the Yellow River, and characterized by typical estuarine features, such as abundance of terrestrial organic matters, lower salinity, and depth. Biotope-C was located at the intertidal and subtidal zone of the southern branch of the Yellow River estuary that was almost blocked in the 1990s. Biotope-D was located at the subtidal zone facing open water and featured deeper water and higher salinity. Biotope-B was located at the intertidal and subtidal zone near the ancient Yellow River estuary facing open water. Biotope-S, which was located at the intertidal and subtidal zone in Laizhou Bay, was closer to the mainland and influenced more by the weaker diluted water from the bottom of Laizhou Bay rather than diluted water from the Yellow River. Five evenly spaced sites were chosen from each biotope for comparison; thus, in total, twenty-five sites were selected for collecting fish specimens for stable isotopic analysis. After the summer fishing moratorium ended in September 2017 and September 2018, a fishing boat trawled at 2 kn for 30 min (Choy et al., 2015) at each site. Specimens were weighed and frozen at -20 °C after species identification. Three

replicates of stable isotope analysis were carried out on each species. Zooplankton specimens were collected as an assemblage of communities using a 200-μm zooplankton net that was horizontally trawled at 2 kn for 10 min. Three replicate samples were taken, filtered using a pump system and 200-μm bolting silk filters, wrapped in foil, placed in sealed bags, and then stored at -20 °C until further analysis. Suspended particulate organic matter (POM), which mainly contained phytoplankton and organic detritus, was collected by filtering seawater through pre-combusted Whatman GF/F glass fiber filters (Kohlbach et al., 2016), and subsequent methods were the same with zooplankton sample collection. Microscopic photosynthetic organisms living on the sediment surface were referred to as microphythobenthos, mainly comprising diatoms and cyanobacteria (Christianen et al., 2017), which compose the sedimental organic matter (SOM) with other organic detritus. SOM specimens were collected using a clam grab bucket. The surface layers (< 5 mm) of the sediment were scraped off, foil-wrapped, and then frozen at -20 °C for further processing. Enteromorpha and spartina were, respectively, collected and then foil-wrapped and frozen as a proxy for macroalgae and cordgrass, because of their dominating position in local biotopes.

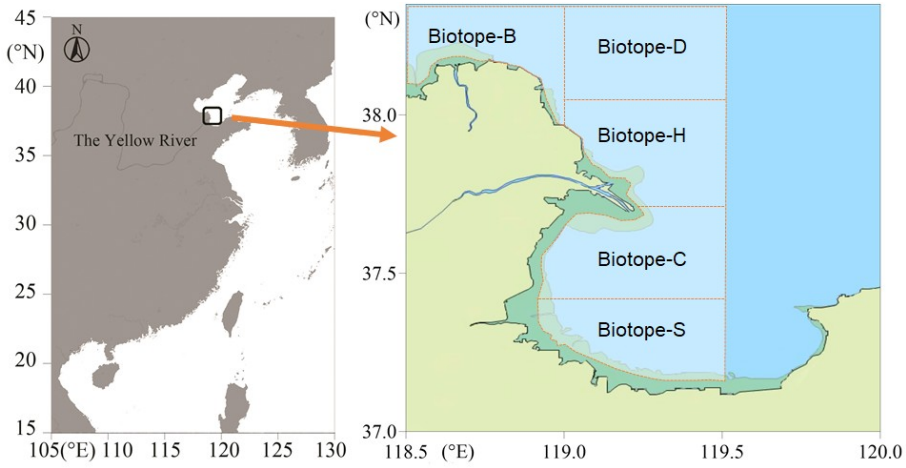

Figure 1. Research area off the Yellow River estuary and adjacent sea areas

Sample treatment and stable isotope analysis

In this study, local dominating fish species (average site biomass > 90%), from the five research biotopes, were collected for $\delta^{13}C$ and $\delta^{15}N$ analysis. The dorsal muscle tissues of fishes were used for stable isotope analysis, which reflects long-term

information about nutrient accumulation (McIntyre and Flecker, 2006). Mixed zooplankton samples composed of several species were analyzed together to gain nitrogen stable isotope data for the TL baseline (Hoen et al., 2014). Each specimen was separated into two equal quantity samples. One sample was treated with 1 mol/L hydrochloric acid to remove inorganic carbon for $\delta^{13}C$ analysis (Kanaya et al., 2007), while the non-acidified one was used directly for $\delta^{15}N$ analysis. All samples were oven dried for approximately 24 to 48 h at 70 °C until a constant weight was achieved, and then homogenized into uniform particle size powder using a triturator. After pretreatment, the main process of carbon and nitrogen isotopic analysis was performed using an isotope ratio mass spectrometer (Delta V™, Thermo Fisher, Germany). Stable isotope ratios were expressed in standard δ unit notation ($\delta^{13}C$ and $\delta^{15}N$), and defined as follows:

$$\delta^{13}C(‰) = \left(\frac{^{13}C/^{12}C_s}{^{13}C/^{12}C_{VPDB}} - 1\right) \times 1000 \quad (1)$$

$$\delta^{15}N(‰) = \left(\frac{^{15}N/^{14}N_s}{^{15}N/^{14}N_{air}} - 1\right) \times 1000 \quad (2)$$

where $^{13}C/^{12}C_s$ and $^{15}N/^{14}N_s$ are the ratios of heavy isotopes to light isotopes from the samples and $^{13}C/^{12}C_{VPDB}$ and $^{15}N/^{14}N_{air}$ are the Vienna Pee Dee Belemnite (VPDB) standard and atmospheric N_2 standard for ^{13}C and ^{15}N, respectively (Jeglinski et al., 2013).

Data analysis

$\delta^{13}C$ and $\delta^{15}N$ were analyzed using the current most efficient procedures, including SIBER metrics (Stable Isotope Bayesian Ellipses in R version 3.6.1), SIAR package (Stable Isotope Analysis in R), IsoSource (Phillips et al., 2012, www.epa.gov/wed/pages/ models.htm), and the TL model (Post, 2002; Du et al., 2020). SPSS Statistics Subscription (IBM Inc., Armonk, NY, USA) was also used to determine how similar isotopic signatures were, and to distinguish the sources of identical stable isotope characteristics.

Isotopic niche analysis

SIBER is a multivariate ellipse-based model available in an R statistical computing package, which can reformulate metrics in a Bayesian framework for direct comparison of isotopic niches across biocoenosis (Jackson et al., 2011). When comparing individual groups with each other, either within a single community or in groups of communities, the Standard Ellipse Area (SEA) was recommended by the program author. With the SIBER object created, isotope biplots could be displayed using stated functions, and some summary statistics could be calculated for each group in the dataset. In this study, a pairwise comparison of biotopes was implemented using SIBER. The stable isotopic niche areas of each group, which were determined by the SEA, represented the trophic niche of respective fish communities plotted on a $\delta^{13}C$-$\delta^{15}N$ dot plot. The ellipse area corrected for the small sample size (SEAc) and the stable isotopic niche width of each fish community was computed for comparison.

Trophic level calculation

Seven common fish species were collected to calculate and compare their TLs in each biotope. TLs were determined based on the nitrogen isotopic fractionation for ^{15}N enrichment through the food chains considering the consumer ingestion and metabolic process (Caut et al., 2009, 2010), undergoing predictable changes with each successive level up the trophic ladder (Smit et al., 2005). The recognized trophic fractionation factor of $\delta^{15}N$ ($\Delta^{15}N$) was 3.4‰ between contiguous TLs (Post, 2002). TLs could be calculated using the traditional model formula, as follows:

$$TL = TL_{base} + \frac{\delta^{15}N_c - \delta^{15}N_b}{\Delta^{15}N} \quad (3)$$

where TL is the consumer trophic level, TL_{base} is the baseline trophic level, $\delta^{15}N_c$ is the consumer nitrogen isotope ratio, $\delta^{15}N_b$ is the marine primary consumer nitrogen isotope ratio, and $\Delta^{15}N$ is the trophic fractionation factor. Primary consumers occupied the 2nd TL at the base of the trophic ladder, so the $\delta^{15}N$ value of zooplankton was considered the baseline in this study.

Food source analysis

In this study, we identified five paralic organisms as the original food sources, including autochthonous primary producers (phytoplankton and microphytobenthos) and allochthonous food sources (macroalgae, cordgrass, and organic matter from the Yellow River (YROM)), which were the primary energy providers for local paralic food webs, as the potential primary food sources of fish species, analyzed the contributions of each potential food source using IsoSource and SIAR, and then drew block diagrams illustrating the results with SIAR. According to Wang et al. (2018), estuarine organic matter is predominately from autochthonous sources, and the estimated autochthonous organic carbon is approximately 58 to 82% of total organic carbon. Therefore, POM with a diameter between 20 and 200 μm was deemed representative of estuarine-marine phytoplankton and the associated isotope values were used in food source analysis. Surface SOM (< 5 mm) excluded inorganic carbon and was represented by microphytobenthos in local research areas. Enteromorpha and spartina were represented by macroalgae and cordgrass in the subtidal and intertidal zone, respectively. Since the diluted water directly influenced Biotope-H and Biotope-C more than Biotope-B, Biotope-D, and Biotope-S, YROM in Biotope-H and Biotope-C was included in the food source analysis, while that in Biotope-B, Biotope-D, and Biotope-S was not. The results from previous study indicated that there was no significant difference between YROM and primary terrestrial vegetation in the Yellow River Delta (Qu et al., 2019), so YROM was suitable for representing delta vegetation in a local finite area. Consequently, five potential food sources were identified in Biotope-H and Biotope-C, corresponding to a 20% average contribution for fish species, while four potential food sources corresponding to a 25% average contribution were identified in Biotope-B, Biotope-D, and Biotope-S. The contribution of each potential carbon source to fish communities was estimated using SIAR (Jackson et al., 2009 and 2011), while the contribution of each potential carbon source to the seven fish species was analyzed using IsoSource (Philips et al., 2012).

Results

Variation in $\delta^{13}C$ and $\delta^{15}N$

Seventeen common fish species involving 168 specimens were randomly collected from the five local research biotopes using a consistent sampling method for $\delta^{13}C$ and $\delta^{15}N$ analysis (Biomass proportions are shown in Appendix Table S1). The average $\delta^{13}C$ values for each species in the five survey areas are shown in Table 1. Biotope-H was located at the subtidal zone of the northern Yellow River estuary, and was affected most by the abundant diluted water from the Yellow River. In our study, $\delta^{13}C$ values for fish in this biotope had the broadest range, from -22.17‰ to -16.94‰ with an average of -19.52‰. Biotope-C was located at the subtidal zone of the southern Yellow River estuary, where the effect of diluted water was weaker than the northern area because of silting at the southern river mouth. The $\delta^{13}C$ values for fish here ranged from -21.50‰ to -17.48‰ with an average of -19.63‰. Biotope-D , which was located further north of the Yellow River estuary, approaching open water, had less of a diluted water effect. The $\delta^{13}C$ values for fish here ranged from -23.30‰ to -20.00‰ and the average was -21.40‰. Biotope-B, located at the edge of the intertidal zone northwest of the Yellow River estuary, was strongly influenced by local diluted water from river branching rather than the Yellow River mainstream. The $\delta^{13}C$ values for fish here ranged from -19.80‰ to -17.87‰ and the average was -18.87‰. For Biotope-S, which was located near the intertidal zone of Laizhou Bay, south of the Yellow River, the most influential factor was local land input instead of diluted water from the Yellow River. The $\delta^{13}C$ values for fish here ranged from -21.56‰ to -18.68‰ with an average of -20.02‰.

The average $\delta^{15}N$ values are shown in Table 2. Similar to $\delta^{13}C$ values, the $\delta^{15}N$ range for fish in Biotope-H was the broadest, from 7.05‰ to 14.30‰ with an average of 12.08‰. The $\delta^{15}N$ for fish in Biotope-B ranged from 10.62‰ to 13.16‰ with an average of 11.97‰. The $\delta^{15}N$ for fish in Biotope-D ranged from 10.08‰ to 13.12‰ with an average of 11.57‰. The $\delta^{15}N$ for fish in Biotope-C ranged from 10.20‰ to 15.28‰ with an average of 12.57‰, and the $\delta^{15}N$ for fish in Biotope-S ranged from 11.89‰ to 17.09‰ with an average of 14.80‰. The $\delta^{15}N$ data for Biotope-S were significantly higher than all other biotopes ($P < 0.01$), while the $\delta^{15}N$ data for Biotope-C were significantly higher than those for Biotope-B and Biotope-D ($P < 0.05$, Appendix Table S2).

264

Table 1. $\delta^{13}C$ (mean values ± SD, n = 3) of seventeen fish species in five survey areas in 2017 and 2018

No.	Species	B: $\delta^{13}C$ (‰)	D: $\delta^{13}C$ (‰)	H: $\delta^{13}C$ (‰)	C: $\delta^{13}C$ (‰)	S: $\delta^{13}C$ (‰)
1	*Argyrosomus argentatus*	-18.02 ± 0.03	-20.70 ± 0.78	-19.31 ± 0.32	-18.27 ± 0.72	-20.87 ± 0.24
2	*Konosirus punctatus*	-18.70 ± 0.06	-21.33 ± 0.64	-19.90 ± 0.13	-19.36 ± 0.06	-21.09 ± 0.03
3	*Cynoglossus semilaevis*	-19.01 ± 0.30	-20.60 ± 0.78	-19.02 ± 0.38	-19.71 ± 0.41	-19.38 ± 0.26
4	*Thryssa kammalensis*	-19.19 ± 0.26	-20.80 ± 0.70	-22.01 ± 0.24	-20.88 ± 0.55	-20.34 ± 1.06
5	*Amblychaeturichthys hexanema*	-19.70 ± 0.07	-20.57 ± 0.81	-20.42 ± 0.43	-19.52 ± 0.70	-19.11 ± 0.00
6	*Sardinella zunasi*	-19.14 ± 0.12	-21.77 ± 0.90	-20.20 ± 0.30	-19.69 ± 0.54	-20.95 ± 0.32
7	*Platycephalus indicus*	-18.49 ± 0.07	-22.97 ± 0.21	-19.20 ± 0.09	-19.66 ± 0.07	-19.11 ± 0.71
8	*Synechogobius hasta*	-18.35 ± 0.31	-20.87 ± 0.72	-20.14 ± 0.34	-19.25 ± 0.23	—
9	*Triaenopogon barbatus*	-19.38 ± 0.50	-21.27 ± 0.67	—	—	—
10	*Thryssa mystax*	-19.29 ± 0.51	—	-20.16 ± 0.82	-20.15 ± 0.29	—
11	*Cynoglossus joyneri*	-18.28 ± 0.36	—	-17.60 ± 0.81	—	—
12	*Enedrias fangi*	—	-23.10 ± 0.20	—	—	—
13	*Sillago japonica*	—	—	-18.99 ± 0.48	—	—
14	*Eupleurogrammus muticus*	—	—	-19.58 ± 0.04	—	—
15	*Odontamblyopus rubicundus*	—	—	-18.28 ± 0.01	-19.79 ± 0.01	—
16	*Setipinna tenuifilis*	—	—	-18.44 ± 0.37	-19.72 ± 1.27	-19.39 ± 0.22
17	*Pampus echinogaster*	—	—	-19.61 ± 0.30	—	-19.93 ± 0.19

272Table 2. $\delta^{15}N$ (mean values ± SD, n = 3) of seventeen fish species in five survey areas in 2017 and 2018

No.	Species	B: $\delta^{15}N$ (‰)	D: $\delta^{15}N$ (‰)	H: $\delta^{15}N$ (‰)	C: $\delta^{15}N$ (‰)	S: $\delta^{15}N$ (‰)
1	*Argyrosomus argentatus*	12.96 ± 0.04	11.15 ± 0.82	12.70 ± 1.21	12.58 ± 0.57	15.36 ± 0.77
2	*Konosirus punctatus*	11.24 ± 0.22	11.76 ± 0.89	10.97 ± 0.53	10.38 ± 0.16	11.93 ± 0.07
3	*Cynoglossus semilaevis*	11.31 ± 0.60	10.84 ± 0.90	12.16 ± 0.48	12.36 ± 0.30	13.58 ± 0.06
4	*Thryssa kammalensis*	11.80 ± 0.08	11.27 ± 0.85	12.57 ± 0.06	13.66 ± 0.31	14.94 ± 0.14
5	*Amblychaeturichthys hexanema*	11.62 ± 0.23	10.75 ± 0.94	12.18 ± 0.10	12.39 ± 0.25	15.75 ± 0.17
6	*Sardinella zunasi*	13.01 ± 0.03	11.91 ± 0.84	7.89 ± 0.80	11.46 ± 0.97	15.89 ± 0.09
7	*Platycephalus indicus*	12.30 ± 0.58	12.07 ± 0.56	13.48 ± 0.24	13.57 ± 0.30	14.09 ± 0.03
8	*Synechogobius hasta*	10.98 ± 0.07	11.47 ± 0.51	13.52 ± 0.01	12.70 ± 0.58	—
9	*Triaenopogon barbatus*	11.91 ± 0.06	11.53 ± 0.82	—	—	—
10	*Thryssa mystax*	11.52 ± 0.26	—	11.52 ± 0.17	11.95 ± 0.25	—
11	*Cynoglossus joyneri*	13.03 ± 0.12	—	13.52 ± 0.45	—	—
12	*Enedrias fangi*	—	12.99 ± 0.11	—	—	—
13	*Sillago japonica*	—	—	9.79 ± 0.56	—	—
14	*Eupleurogrammus muticus*	—	—	11.82 ± 0.83	—	—
15	*Odontamblyopus rubicundus*	—	—	12.40 ± 0.67	12.26 ± 0.03	—
16	*Setipinna tenuifilis*	—	—	13.85 ± 0.41	14.90 ± 0.41	14.69 ± 0.16
17	*Pampus echinogaster*	—	—	12.81 ± 0.42	—	16.94 ± 0.15

274

275

Comparing stable isotopic niches using SIBER

Biotope-H was most influenced by diluted water from the Yellow River, so it was chosen as the object of comparison with the other biotopes (B, D, C, and S), avoiding too complex and mixed-up dots with their SEA in a single plot using SIBER (Figure 2). The niche width of $\delta^{13}C$ and $\delta^{15}N$ for fish is shown in Table 3. In Biotope-H, the niche width of $\delta^{13}C$ and $\delta^{15}N$ was 7.24 and 5.24, respectively, and both had the widest niche of all selected biotopes (Table 3). Niche widths in Biotope-B were the narrowest at 1.93 for $\delta^{13}C$ and 2.53 for $\delta^{15}N$. Accordingly, Biotope-H had the highest SEAc of 45.38 followed by Biotope-S (4.10) and Biotope-C (2.98), while Biotope-B had the lowest SEAc of 1.36. The isotopic niche area of Biotope-H contained Biotope-B (Figure 2A), while similarly Biotope-H almost included Biotope-C except for one dot (Figure 2C, $\delta^{13}C$ of -21.18, $\delta^{15}N$ of 14.96). The SEAc of Biotope-D was 2.83, and its $\delta^{13}C$ value was significantly lower than that of Biotope-H (t-test, $P < 0.01$, n = 33) (Figure 2B). The SEAc of Biotope-S was 4.10, and its $\delta^{15}N$ was significantly higher than that of Biotope-H (t-test, $P < 0.01$, n = 27) (Figure 2D).

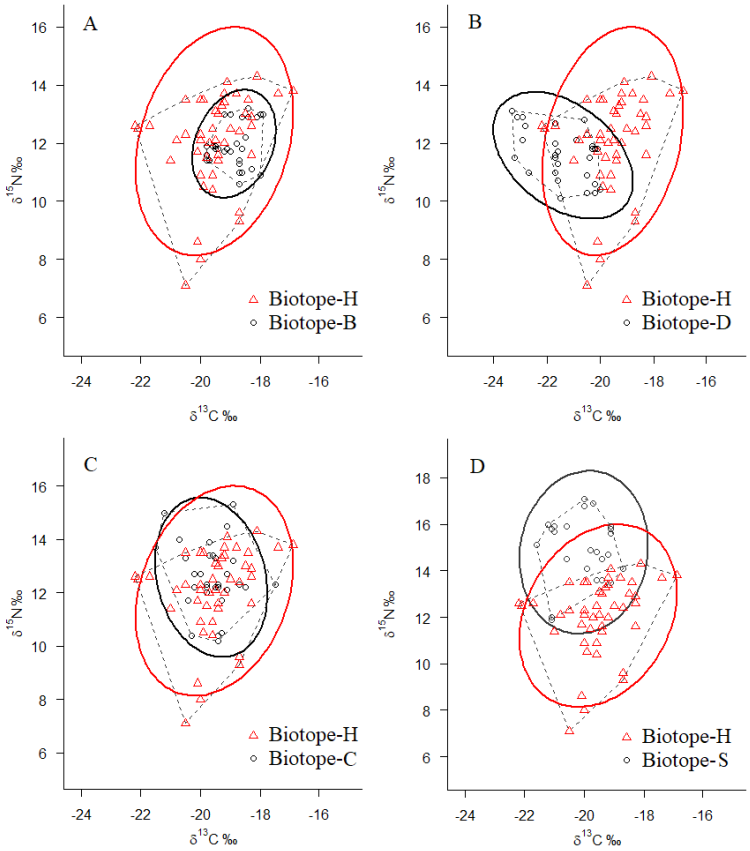

Figure 2. A dot plot of $\delta^{13}C$-$\delta^{15}N$ with the standard ellipse area (SEAc) illustrating comparisons between Biotope-H and other biotopes (Biotope-B, Biotope-D, Biotope-C, and Biotope-S corresponding to inset A, B, C and D, respectively) using the SIBER package. (Biotope-H was drawn as red triangles, and the other biotopes were drawn as black circles)

Table 3. Sampling number (n), niche width ($\delta^{13}C$ and $\delta^{15}N$) and SIBER analysis results including the total area (TA), standard Bayesian Ellipse Area (SEA), and ellipse area corrected for small sample size (SEAc) in five different biotopes.

Biotopes	n	$\delta^{13}C$ niche width	$\delta^{15}N$ niche width	TA	SEA	SEAc
B	33	1.93	2.53	3.68	1.32	1.36
D	30	3.30	3.04	7.38	2.73	2.83
H	45	5.24	7.24	20.27	5.26	5.38
C	33	4.02	5.08	13.36	2.89	2.98
S	27	2.88	5.21	9.35	3.94	4.10

Trophic levels

As seven common fish species (*Argyrosomus argentatus, Amblychaeturichthys hexanema, Cynoglossus semilaevis, Thryssa kammalensis, Konosirus punctatus, Platycephalus indicus,* and *Sardinella zunasi*) appeared in all five biotopes, they were chosen for TL and food source comparisons in this study. The TLs of these seven species in each biotope were calculated using a unique baseline. Figure 3 shows the average TL of the seven representative fishes in each biotope. Agreeing with $\delta^{15}N$ data, the highest average TL of 4.0 was found for Biotope-S, while the lowest average of 3.1 was found for Biotope-D. The TL of Biotope-S was significantly higher than any other biotope ($P < 0.01$, Appendix Table S3). Biotope-H had the highest standard deviation (0.5), while Biotope-D had the lowest standard deviation (0.2). For single species, the highest TL was 4.5 (*Sardinella zunasi*) in Biotope-S, while the lowest TL was 2.1 (also *Sardinella zunasi*) in Biotope-H.

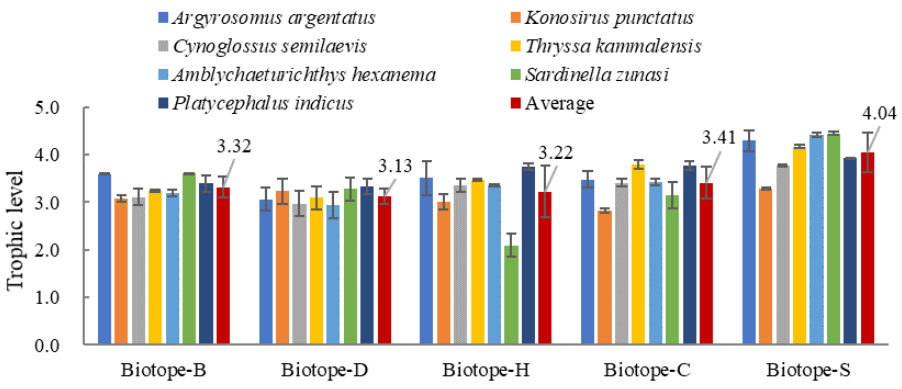

318

319Figure 3. TLs of the seven common fish species (average labeled) in the five biotopes

320**Food source analysis**

321As shown in Figure 4, the contribution of the five potential food sources showed a 322similar distribution tendency in Biotope-H and Biotope-C (Appendix Table S4). 323Allochthonous food sources (macroalgae, cordgrass, and YROM) showed higher 324proportional contributions to local fish communities than autochthonous sources 325(POM and SOM) (Figure 4). The 95% confidence intervals (CIs) were 0.01 to 0.44 for 326macroalgae, 0.04 to 0.43 for cordgrass, and 0.10 to 0.40 for YROM, and 0 to 0.37 for 327POM and 0 to 0.24 for SOM in Biotope-H. The 95% CIs were 0 to 0.47 for 328macroalgae, 0.03 to 0.44 for cordgrass, and 0.17 to 0.43 for YROM, and 0 to 0.37 for 329POM and 0 to 0.12 for SOM in Biotope-C. The 95% CIs for macroalgae showed the 330widest distribution, which was 0.43 in Biotope-H and 0.47 in Biotope-C, respectively. 331YROM demonstrated less variation in the confidence interval, which was 0.30 in 332Biotope-H and 0.16 in Biotope-C. Conversely, SOM showed the lowest contribution, 333with a 95% CI of 0 to 0.24 in Biotope-H and 0 to 0.12 in Biotope-C, respectively. For 334single species, both macroalgae and cordgrass contributed relatively more to 335*Argyrosomus argentatus* (mean = 0.33 and 0.30 in Biotope-H; 0.32 and 0.33 in 336Biotope-C), while YROM contributed a 0.37 mean proportion for *Thryssa* 337*kammalensis* in Biotope-H. More detailed food source contribution data for fish 338species are shown in Appendix Table S4 and S5.

339In Biotope-D, which was the farthest offshore, POM showed a significantly higher 340food source contribution, and its 95% CI was higher (0.26 to 0.79) than any other 341potential food sources (Figure 5, Appendix Table S4), and for single species, the 342highest mean contribution of POM was to *Konosirus punctatus* (0.76) in Biotope-D 343(Appendix Table S5). The 95% CI for SOM was also higher (0.17 to 0.53) than for 344macroalgae and cordgrass, which showed extremely low 95% CIs of 0 to 0.18 and 0

to 0.11, respectively. In Biotope-S, POM and SOM were also considered to be the primary food sources based on contribution results, which accounted for 0 to 0.61, but with high distribution indeterminacy (0.61), and 0.16 to 0.54 for 95% CIs, respectively. In Biotope-B, the contributions of each food source were in relative equilibrium, while for single species, cordgrass showed a 0.48 contribution to *Argyrosomus argentatus* (Appendix Table S5).

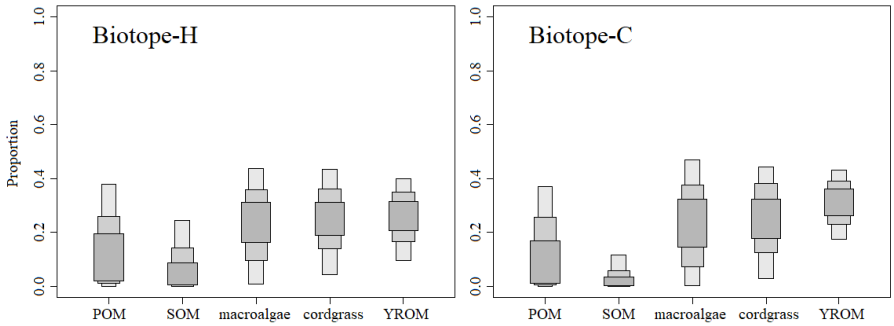

Figure 4. Relative contribution of the five potential food sources to the diet of fish communities in Biotope-H and Biotope-C using SIAR. Grey shaded areas represent 95%, 75%, and 50% confidence intervals. (Food source containing POM = suspended particulate organic matter, SOM = sedimental organic matter, macroalgae, cordgrass, and YROM = Yellow River organic matter.)

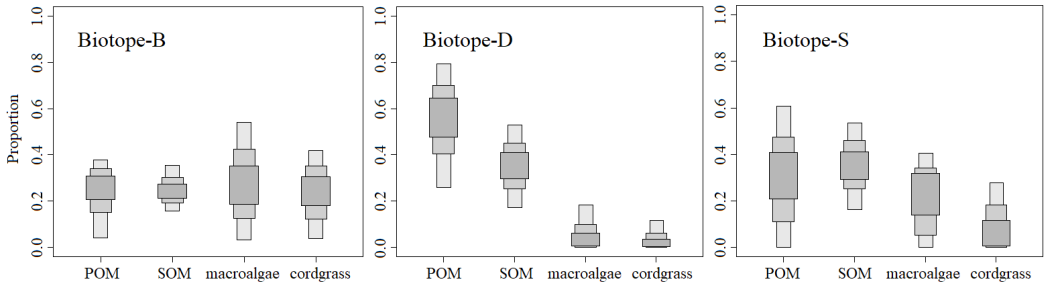

Figure 5. Relative contribution of the five potential food sources to the diet of fish communities in Biotope-B, Biotope-D, and Biotope-S using SIAR. Grey shaded areas represent 95%, 75%, and 50% confidence intervals. (Food source containing POM = suspended particulate organic matter, SOM = sedimental organic matter, macroalgae and cordgrass.)

Discussion

Trophic niche variation

Increasing numbers of studies have shown that coastal and estuarine ecological connectivity plays an essential role in ecosystem conservation and restoration (Du et al., 2015). The stable isotopic niche results in this study indicated that the SEAc (5.38) and total area (TA, 20.27) of estuarine Biotope-H covered the majority of the other research areas (Figure 2, Table 3). In general, the results showed the compatibility of communities among Yellow River estuarine habitants, and that the area may be a corridor for energy and material transportation between Laizhou Bay and the open water. Further, the results highlight the importance of terrestrial-marine linkages for interpreting energy flow in estuarine ecosystems (Wai et al., 2011). Local biocoenosis used various food sources to adapt to the fickle environment, including marine-terrestrial boundaries and the estuary, and this was embodied in the wider isotopic niche corresponding to frequent environmental changes and abiotic gradients (Lange et al., 2018). These marine-terrestrial linkages served as feeding and nursery grounds for fish biocoenosis, where even top predators like shark species gained trophic subsidies along food chains from land (Wai et al., 2012). A comparative analysis of stable isotopic niches was useful for detecting patterns in trophic structure and identifying differences or similarities in trophic organization related to environmental conditions (Abrantes et al., 2014). It is evident that changes to the TLs and food sources of fish communities in terms of $\delta^{13}C$ and $\delta^{15}N$ will have an effect on conservation.

The $\delta^{13}C$ data in our study indicated that all fish species were mainly corresponding to benthic diatoms, macroalgae, and estuarine-marine phytoplankton (Cloern et al., 2002), which occupy normal marine isotopic niches (Newsome et al., 2007). Beyond macroalgae, our analysis of the food source contribution indicated that YROM and cordgrass were major allochthonous energy sources in estuarine areas directly affected by Yellow River-diluted water, while local autochthonous primary producers (phytoplankton and microphytobenthos) demonstrated a low contribution in those specific areas (Figure 4). Phytoplankton produce new particles that drive the biological carbon pump, contributing to the global carbon cycle in the ocean, which plays a disproportionately important role in the global climate on a range of time scales (Bolaños et al., 2020; Moreau et al., 2020). However, it is susceptible to

environmental conditions relative to other primary producers, especially the variable environment of estuaries. The bloom and extinction of phytoplankton is driven by physical, chemical, and biological seasonality (Bolaños et al., 2020). Hydrology and dissolved nutrients have been widely identified as the main drivers of phytoplankton dynamics in estuarine ecosystems (Tao et al., 2020). Our investigation indicated that a high concentration of chlorophyll-a, a representative of phytoplankton (Moreau et al., 2020), had not shown up in estuarine areas with a direct diluted water influence (Appendix 1). This is consistent with the results of Ding et al. (2020). Microphytobenthic primary producers also demonstrated a low contribution, probably due to their dependency on light (Haro et al., 2019) and encounter with high-suspended solids (Wang et al., 2017). On the other hand, besides macroalgae, allochthonous energy sources were identified as the main food sources supporting the estuarine food web. In a previous study, most of the riverine organic carbon originated from delta vegetation debris (Phragmites, Suaeda, and Tamarisk) in particulate form (Wang et al., 2018). Suspended particulate matter acts as the main carrier of organic matter, providing energy to the estuarine food web from upstream carrying, which plays an important role in the conditioning of productivity and ecosystem functions in estuaries (Li et al., 2020). As a representative of cordgrass in the intertidal zone, spartina provided a considerable food contribution proportion for estuarine fish communities in this study. However, it was recognized as the main invasive plant in the Yellow River estuarine area, so its contribution to the local estuarine food web is still controversial (Chen et al., 2020). *Spartina alterniflora* was first introduced to the coastal wetlands of China from the United States in 1979 for the purpose of ecological restoration. From 1985 to 2015, it continued to spread across the coast of mainland China as a typical invasive species (Meng et al., 2020).

Areas away from the Yellow River estuary show different food contribution characteristics compared with the estuarine area. As indicated by the food source contribution results, autochthonous benthic and pelagic producers (microphytobenthos and phytoplankton) dominated carbon input into the food web in Biotope-S and Biotope-D, which conformed to the normal characteristics of an intertidal ecosystem like the Wadden Sea (Christianen et al., 2017). Microphytobenthos form extensive biofilms on the sediment surface conducive to its stabilization. They are not easily disturbed and thus provide a more stable food source for local consumers (Hart and Lovvorn, 2003; Miyatake et al., 2014). In contrast, phytoplankton are more vulnerable to influence from environmental conditions (Armbrecht et al., 2015), while providing

an unstable food source according to the more discrete confidence interval of contribution (Figure 5).

Majorization of the trophic model baseline

The $\delta^{15}N$ data indicated that the fish species in our study system belonged to TL 2.1 to 4.5 using a unique baseline (Figure 3), covered a TL distance of 2.4, which differed from the general trophic pattern of fish communities in Chinese coastal waters, such as 3.0 to 4.1 for Changjiang Estuary at the junction of the Yellow Sea and the East China Sea (Chang et al., 2014), 3.1 to 3.6 in the coastal water of the Yellow Sea (Feng et al., 2014), and 2.9 to 3.9 at the junction of the East China Sea and South China Sea (Du et al., 2015). Their trophic niche was also wider than that in the western Mediterranean (2.9 to 4.0, Valls et al., 2014), but lower than that in the Gulf of Maine (3.7 to 5.2, Schartup et al., 2019). From the above comparisons, the variation in TL in our research area (2.4) was much wider than in other similar coastal areas. Intriguingly, this variation was reflected not only in single species, but also significantly in the biotopes according to the results of this study (Appendix Table S3). Our results demonstrated that the average fish TL was 3.3 in Biotope-B, 3.1 in Biotope-B, 3.2 in Biotope-H, 3.4 in Biotope-C, and 4.0 in Biotope-S, giving the trend of S > C > B > H > D. This tendency showed that the average TL was significantly higher in Laizhou Bay than any other biotope and decreased from the near shore biotope to the far shore, which meant significant variation in our original $\delta^{15}N$ data. It was an abnormal phenomenon that similar species had such a significantly different $\delta^{15}N$ characteristic between connected biotopes.

$\delta^{15}N$ can also be used to indicate scenopoetic dimensions, such as marine-terrestrial (Lange et al., 2018) and eutrophication (Gooddy et al., 2016). Generally, the difference in habitat conditions is mainly related to the scenopoetic dimensions where a high $\delta^{15}N$ value indicate a marine characteristic while a low value indicate a terrestrial characteristic; a high value also indicates a eutrophic area while a low value indicates a pristine area (Newsome et al., 2007). The environmental condition of Laizhou Bay is closer to a mainland and it belongs more to a terrestrial rather than a marine characteristic with its lower $\delta^{15}N$ value, and thus the results in our study did not obey the marine-terrestrial pattern. We also suspected that local aquaculture activities might lead to a high $\delta^{15}N$ value from wild marine lives by releasing organic bait based on similar conditions in the aquaculture water in Jiaozhou Bay, off the coast of China (Feng et al., 2014). Therefore, a field survey was conducted in May

2020 and scallop culture was identified as the main local aquaculture with no release of anthropogenic organic bait. After excluding the above conditions, we needed a more reasonable theory to explain the abnormal phenomenon in our study area.

After the above analysis, we turned our attention to probing into the $\delta^{15}N$ variation based on the food source contribution. Whether in a high $\delta^{15}N$ (Biotope-S) or low $\delta^{15}N$ (Biotope-D) area, the autochthonous food source demonstrated a relatively high contribution to the local fish communities, which implied that it is probably due to the influence of primary producers at the base of the food web (Oakes et al., 2010). However, primary producers seldom directly provide energy to high-TL predators (Warne et al., 2010), so it does not adequately explain the $\delta^{15}N$ variation in different biotopes. Therefore, in May 2020, we reanalyzed the zooplankton, which was considered a mediator of energy-transfer from primary producers to high-TL predators and tended to respond to variations in food source $\delta^{15}N$ values (Schmidt et al., 2003), and then recalculated the TL of fishes using zooplankton $\delta^{15}N$ values as the baseline in each biotope (Figure 6). Compared with the unique baseline, the differences in fish TLs were smaller between each biotope (Figure 6 TL_b). The fish TL in Biotope-C was no longer significantly higher than that in Biotope-B and Biotope-D. Though the fish TL in Biotope-S was still significantly higher than that in the other biotopes, the gaps decreased from 0.83 to 0.42 with Biotope-B, from 0.95 to 0.69 with Biotope-D, from 0.80 to 0.33 with Biotope-H, and from 0.65 to 0.39 with Biotope-C (Appendix Table S6). However, the bias caused by abnormally high $\delta^{15}N$ still existed in the optimized results. This method demonstrated a method for solving the disparity generated from $\delta^{15}N$ data in spatial distribution, which implied a tendency that the $\delta^{15}N$ variation originated in a more fundamental part of the estuarine food web, such as nitrogen cycling dynamics (Hetherington et al., 2017).

To exclude possible error introduced during the calculating process, we also used Hussey's equation to recalculate the TL (Hussey et al., 2014; Reum et al., 2015, method in Appendix 2). Based on the new equation, there were some changes in the TL results, but they still retained the same trend in terms of the average biotope TL (Figure 6, TL_n).

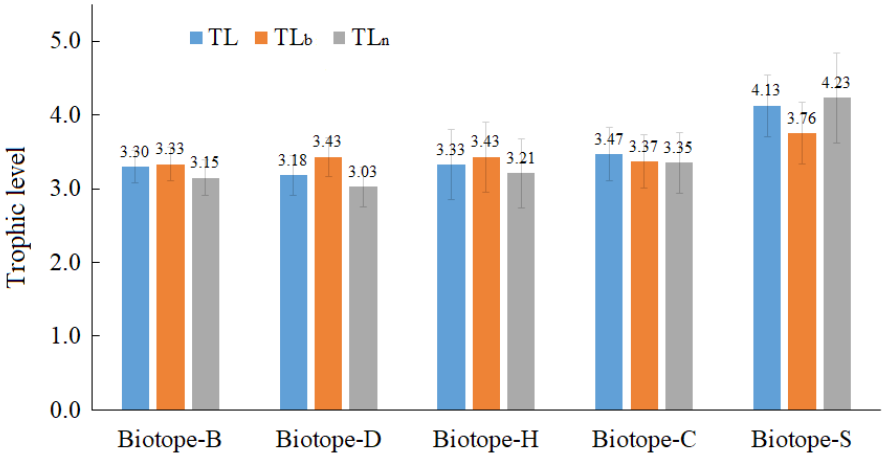

498

499Figure 6. Average TLs of fishes in each biotope using Post's (TL) and Hussey's (TL_n) 500methods, and revised TLs using a different baseline value ($\delta^{15}N$ of primary 501consumers) Post's method (TL_b)

502

503The inorganic nitrogen assimilation process is a key driver from primary producers in 504the marine nitrogen cycle (Hetherington et al., 2017). Due to the high and stable 505contribution for fishes, SOM was considered a primary food source in Biotope-S. We 506further investigated its $\delta^{15}N$ distribution (Figure 7) and found a strong link between 507the high $\delta^{15}N$ of fish and the distribution of dissolved inorganic nitrogen (DIN) 508(Appendix 3). Nitrogen-fixing microorganisms, such as nitrospinae, were also 509significantly enriched in ^{15}N under conditions of a high inorganic nitrogen 510concentration (Kitzinger et al., 2020). Therefore, the high $\delta^{15}N$ value of SOM was 511most probably caused by microorganisms and other primary producers assimilating 512high-concentration DIN, which was likely the reason for the eutrophic pattern of $\delta^{15}N$ 513(Newsome et al., 2007). The major primary consumers, zooplankton, tended to 514respond to this variation (Schmidt et al., 2003). This characteristic would translate to 515high-TL consumers like fish communities via marine food chains leading to biases in 516the statistical process (Auerswald et al., 2010; Layman et al., 2012).

517

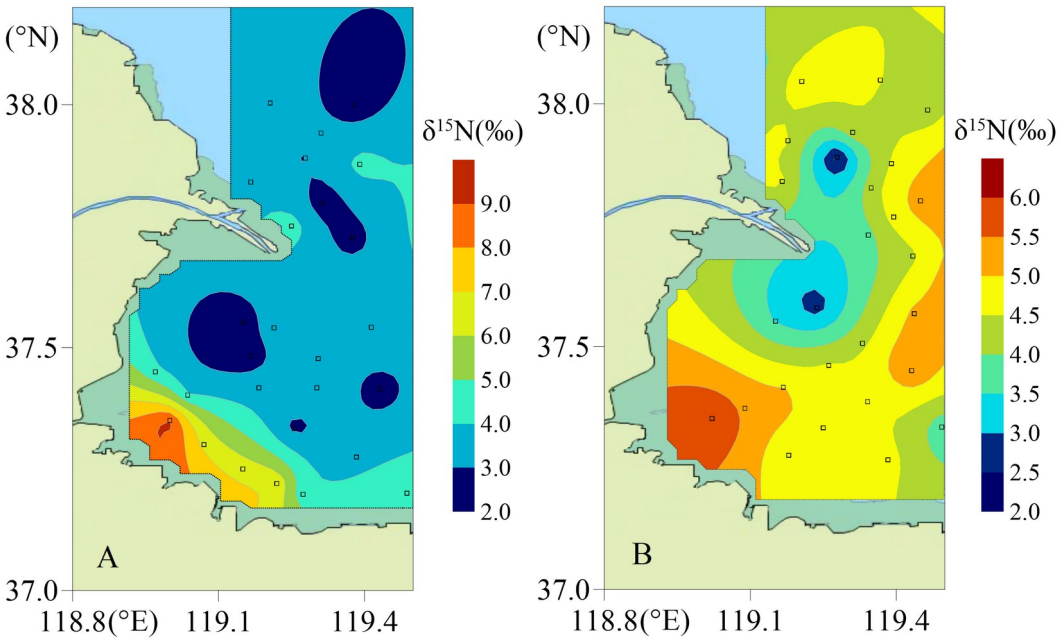

Figure 7. The distribution of $\delta^{15}N$ in organic sediment in August 2017 (A) and May 2020 (B).

Hetherington et al. (2017) used linear mixed effects models (LMEs) to verify that source amino acid $\delta^{15}N$ values in marine lives were related to nitrate concentrations, which pertained to fluctuations in biogeochemical cycling at the base of the food web. Therefore, if we intend to solve this issue fundamentally, the baseline should be optimized through comprehensive and integrated analysis in further research. This conclusion will also promote our next step research with more specific verification to explain the integrated transfer process. Although this conclusion connected a series of transfer processes from high concentration DIN to primary producers, to primary consumers, and then to higher consumers like fishes, which were so complicated and contained too many intermediate processes, it is the most likely reason to explain this abnormal phenomenon based on a previous theory (Teichberge et al., 2010; Kitzinger et al., 2020) combined with our results, which suggested highly connected food web loops.

Many previous studies found that their application was further complicated by potential shifts in baseline $\delta^{15}N$ for many specific ecological processes, such as migration of marine nektons like bluefin tuna and swordfish (Schartup et al., 2019), significant taxonomic variation in the composition of primary producers at the base of the food webs (Ramshaw et al., 2017), and supply way of DIN sources (Kitzinger et al., 2020). The $\delta^{15}N$ characteristic of primary producers may vary by as much as 10‰ over a spatial and temporal scale (McMahon et al., 2015). Therefore, identifying an

appropriate baseline requires not only considering migratory predators but also paying more attention to the local primary producers that can determine the baseline of marine trophic structures more directly.

If our conclusion is right that the local high $\delta^{15}N$ of fishes originated from the high concentration of DIN in Biotope-S, a trophic model relying on the $\delta^{15}N$ characteristic would be further complicated by potential shifts in the baseline due to variations in the $\delta^{15}N$ characteristic in primary producers (Gutiérrez-Rodríguez et al., 2014). Regional $\delta^{15}N$ diversity in primary producers should be considered not only between broad oceans on a large spatial scale (Schmidt et al., 2003; Hetherington et al., 2017), but also among adjacent coastal waters with high DIN variation, such as the estuary. Though the research areas in our study were not significantly isolated, the bias of TLs in fish communities still emerged between biotopes, which indicates the diversity of matter and energy flows (Palmer et al., 2019).

Conclusion

Stable isotopic niche results indicated that estuarine habitants showed the compatibility of the communities of most study biotopes, which may provide a corridor for energy and material transportation between Laizhou Bay and the open water. YROM and cordgrass were considered the major allochthonous energy sources in estuarine areas directly affected by Yellow River-diluted water, while phytoplankton and microphytobenthos demonstrated a low contribution as local autochthonous primary producers. Areas away from the Yellow River estuary showed different food contribution characteristics compared with estuarine areas. As indicated by the food source contribution results, autochthonous benthic and pelagic producers (microphytobenthos and phytoplankton) dominated carbon input into food webs. Our results showed that the significant variation in the fish $\delta^{15}N$ characteristic presented within estuarine adjacent regions (less than 2 degrees latitude), led to significant variation in TLs in the same fish species, using a unique baseline. Although the research areas in our study were not significantly isolated, the bias of TLs in fish communities still emerged between biotopes. This indicates the diversity of matter and energy flows. Regional $\delta^{15}N$ diversity in primary producers should be considered not only between broad oceans on a large spatial scale, but also among adjacent coastal waters with high DIN variation. These results offer a new perspective on trophic relationships, and provide the first detailed data for enhancing our understanding of the variations among fish communities in estuarine ecosystems.

Acknowledgement and funding

We thank Xijie Yin's research team of Third Institute of Oceanography, MNR for testing stable isotopic data. This work was supported by National Natural Science Foundation of China (NSFC, Grant Nos. 41706140 and 41606140), China Ocean Mineral Resources R&D Association Project (Grant Nos. DY135-E2-1-02 and DY135-E2-2-05) and Open Fund of Key Laboratory of Ocean Ecological Monitoring and Restoration Technologies, MNR (No: 202004).

Data availability statement

Supporting information is available at online version of the manuscript.

References

Abrantes, K. G., Barnett, A., & Bouillon, S. (2014). Stable isotope-based community metrics as a tool to identify patterns in food web structure in east African estuaries. Functional Ecology, 28(1), 270–282.

Armbrecht, L. H., Thompson, P. a., Wright, S. W., Schaeffer, A., Roughan, M., Henderiks, J., & Armand, L. K. (2015). Comparison of the cross-shelf phytoplankton distribution of two oceanographically distinct regions off Australia. Journal of Marine Systems, 148, 26–38.

Auerswald, K., Wittmer, M. H. O. M., Zazzo, A., Schäufele, R., & Schnyder, H. (2010). Biases in the analysis of stable isotope discrimination in food webs. Journal of Applied Ecology, 47(4), 936–941.

Boecklen, W. J., Yarnes, C. T., Cook, B. A., & James, A. C. (2011). On the Use of Stable Isotopes in Trophic Ecology. Annual Review of Ecology, Evolution, and Systematics, 42(1), 411–440.

Bolaños, L. M., Karp-Boss, L., Choi, C. J., Worden, A. Z., Graff, J. R., Haëntjens, N., … Giovannoni, S. J. (2020). Small phytoplankton dominate western North Atlantic biomass. ISME Journal, 14(7), 1663–1674.

Bukovinszky, T., Frank van Veen, F. J. F., Jongema, Y., & Dicke, M. (2008). Direct and Indirect Effects of Resource Quality on Food Web Structure. Science, 319(5864), 804–807.

Caut, S., Angulo, E., Courchamp, F., & Figuerola, J. (2010). Trophic experiments to estimate isotope discrimination factors. Journal of Applied Ecology, 47(4), 948–954.

608Caut, S., Angulo, E., & Courchamp, F. (2009). Variation in discrimination factors
609 ($\Delta^{15}N$ and $\Delta^{13}C$): The effect of diet isotopic values and applications for diet
610 reconstruction. Journal of Applied Ecology, 46(2), 443–453.
611Chang, N. N., Shiao, J. C., Gong, G. C., Kao, S. J., & Hsieh, C. Hao. (2014). Stable
612 isotope ratios reveal food source of benthic fish and crustaceans along a gradient
613 of trophic status in the East China Sea. Continental Shelf Research, 84, 23–34.
614Chen, M., Ke, Y., Bai, J., Li, P., Lyu, M., Gong, Z., & Zhou, D. (2020). Monitoring
615 early stage invasion of exotic Spartina alterniflora using deep-learning super-
616 resolution techniques based on multisource high-resolution satellite imagery: A
617 case study in the Yellow River Delta, China. International Journal of Applied
618 Earth Observation and Geoinformation, 92(12), 102180.
619Choy, C. A., Popp, B. N., Hannides, C. C. S., & Drazen, J. C. (2015). Trophic
620 structure and food resources of epipelagic and mesopelagic fishes in the north
621 pacific subtropical Gyre ecosystem inferred from nitrogen isotopic compositions.
622 Limnology and Oceanography, 60(4), 1156–1171.
623Christianen, M. J. A., Middelburg, J. J., Holthuijsen, S. J., Jouta, J., Compton, T. J.,
624 van der Heide, T., … Olff, H. (2017). Benthic primary producers are key to
625 sustain the Wadden Sea food web: stable carbon isotope analysis at landscape
626 scale. Ecology, 98(6), 1498–1512.
627Cloern, J. E., Canuel, E. A., & Harris, D. (2002). Stable carbon and nitrogen isotope
628 composition of aquatic and terrestrial plants of the San Francisco Bay estuarine
629 system. Limnology and Oceanography, 47(3), 713–729.
630Curnick, D. J., Carlisle, A. B., Gollock, M. J., Schallert, R. J., & Hussey, N. E. (2019).
631 Evidence for dynamic resource partitioning between two sympatric reef shark
632 species within the British Indian Ocean Territory. Journal of Fish Biology, 94(4),
633 680–685.
634Ding, X., Guo, X., Zhang, C., Yao, X., Liu, S., Shi, J., … Gao, H. (2020). Water
635 conservancy project on the Yellow River modifies the seasonal variation of
636 Chlorophyll-a in the Bohai Sea. Chemosphere, 254, 126846.
637Du, J., Makatipu, P. C., Tao, L. S. R., Pauly, D., Cheung, W. W. L., Peristiwady, T., …
638 Chen, B. (2020). Comparing trophic levels estimated from a tropical marine food
639 web using an ecosystem model and stable isotopes. Estuarine, Coastal and Shelf
640 Science, 233.

641Du, J., Cheung, W. W. L., Zheng, X., Chen, B., Liao, J., & Hu, W. (2015). Comparing
642 trophic structure of a subtropical bay as estimated from mass-balance food web
643 model and stable isotope analysis. Ecological Modelling, 312, 175–181.
644Feng, J.-X., Gao, Q.-F., Dong, S.-L., Sun, Z.-L., & Zhang, K. (2014). Trophic
645 relationships in a polyculture pond based on carbon and nitrogen stable isotope
646 analyses: a case study in Jinghai Bay, China. Aquaculture, 428(5), 258–264.
647Fry, B. (2013). Alternative approaches for solving underdetermined isotope mixing
648 problems. Marine Ecology Progress Series, 472, 1–13.
649Gooddy, D. C., Lapworth, D. J., Bennett, S. A., Heaton, T. H. E., Williams, P. J., &
650 Surridge, B. W. J. (2016). A multi-stable isotope framework to understand
651 eutrophication in aquatic ecosystems. Water Research, 88, 623–633.
652Gutiérrez-Rodríguez, A., Décima, M., Popp, B. N., & Landry, M. R. (2014). Isotopic
653 invisibility of protozoan trophic steps in marine food webs. Limnology and
654 Oceanography, 59(5), 1590–1598.
655Haro, S., Bohórquez, J., Lara, M., Garcia-Robledo, E., González, C. J., Crespo, J. M.,
656 … Corzo, A. (2019). Diel patterns of microphytobenthic primary production in
657 intertidal sediments: the role of photoperiod on the vertical migration circadian
658 rhythm. Scientific Reports, 9(1), 1–10.
659Hart, E. A., & Lovvorn, J. R. (2003). Algal vs. macrophyte inputs to food webs of
660 inland saline wetlands. Ecology, 84(12), 3317–3326.
661Hastie, G. D., Russell, D. J. F., Benjamins, S., Moss, S., Wilson, B., & Thompson, D.
662 (2016). Dynamic habitat corridors for marine predators; intensive use of a coastal
663 channel by harbour seals is modulated by tidal currents. Behavioral Ecology and
664 Sociobiology, 70(12), 2161–2174.
665Hetherington, E. D., Olson, R. J., Drazen, J. C., Lennert-Cody, C. E., Ballance, L. T.,
666 Kaufmann, R. S., & Popp, B. N. (2017). Spatial food-web structure in the eastern
667 tropical Pacific Ocean based on compound-specific nitrogen isotope analysis of
668 amino acids. Limnology and Oceanography, 62(2), 541–560.
669Hoen, D. K., Kim, S. L., Hussey, N. E., Wallsgrove, N. J., Drazen, J. C., & Popp, B.
670 N. (2014). Amino acid 15N trophic enrichment factors of four large carnivorous
671 fishes. Journal of Experimental Marine Biology and Ecology, 453, 76–83.
672Hussey, N. E., Macneil, M. A., Mcmeans, B. C., Olin, J. A., Dudley, S. F. J., Cliff, G.,
673 … Fisk, A. T. (2014). Rescaling the trophic structure of marine food webs.
674 Ecology Letters, 17(2), 239–250.

675Jackson, A. L., Inger, R., Bearhop, S., & Parnell, A. (2009). Erroneous behaviour of
676 MixSIR, a recently published Bayesian isotope mixing model: A discussion of
677 Moore & Semmens (2008). Ecology Letters, 12(3), 1–5.
678Jackson, A. L., Inger, R., Parnell, A. C., & Bearhop, S. (2011). Comparing isotopic
679 niche widths among and within communities: SIBER - Stable Isotope Bayesian
680 Ellipses in R. Journal of Animal Ecology, 80(3), 595–602.
681Jeglinski, J. W. E., Goetz, K. T., Werner, C., Costa, D. P., & Trillmich, F. (2013). Same
682 size - same niche? Foraging niche separation between sympatric juvenile
683 Galapagos sea lions and adult Galapagos fur seals. Journal of Animal Ecology,
684 82(3), 694–706.
685Kanaya, G., Takagi, S., Nobata, E., & Kikuchi, E. (2007). Spatial dietary shift of
686 macrozoobenthos in a brackish lagoon revealed by carbon and nitrogen stable
687 isotope ratios. Marine Ecology Progress Series, 345, 117–127.
688Kitzinger, K., Marchant, H. K., Bristow, L. A., Herbold, C. W., Padilla, C. C., Kidane,
689 A. T., … Kuypers, M. M. M. (2020). Single cell analyses reveal contrasting life
690 strategies of the two main nitrifiers in the ocean. Nature Communications, 11(1),
691 767.
692Kohlbach, D., Graeve, M., A. Lange, B., David, C., Peeken, I., & Flores, H. (2016).
693 The importance of ice algae-produced carbon in the central Arctic Ocean
694 ecosystem: Food web relationships revealed by lipid and stable isotope analyses.
695 Limnology and Oceanography, 61(6), 2027–2044.
696Lange, G., Haynert, K., Dinter, T., Scheu, S., & Kröncke, I. (2018). Adaptation of
697 benthic invertebrates to food sources along marine-terrestrial boundaries as
698 indicated by carbon and nitrogen stable isotopes. Journal of Sea Research, 131,
699 12–21.
700Layman, C. A., Araujo, M. S., Boucek, R., Hammerschlag-Peyer, C. M., Harrison, E.,
701 Jud, Z. R., … Bearhop, S. (2012). Applying stable isotopes to examine food-web
702 structure: An overview of analytical tools. Biological Reviews, 87(3), 545–562.
703Li, P., Ke, Y., Wang, D., Ji, H., Chen, S., Chen, M., … Zhou, D. (2020). Human
704 impact on suspended particulate matter in the Yellow River Estuary, China:
705 Evidence from remote sensing data fusion using an improved spatiotemporal
706 fusion method. Science of The Total Environment, 141612.
707Li, S. N., Wang, G. X, Deng, W., Hu, Y. M., & Hu, W. W. (2009). Influence of
708 hydrology process on wetland landscape pattern: A case study in the Yellow
709 River Delta. Ecological Engineering, 35(12), 1719–1726.

710Livernois, M. C., Fodrie, F. J., Heck, K. L., & Powers, S. P. (2019). Emergent
711 intraspecific multiple predator effects shape estuarine trophic dynamics across a
712 gradient of habitat complexity. Journal of Experimental Marine Biology and
713 Ecology, 511, 120–128.
714McIntyre, P. B., & Flecker, A. S. (2006). Rapid turnover of tissue nitrogen of primary
715 consumers in tropical freshwaters. Oecologia, 148(1), 12–21.
716McMahon, K. W., Thorrold, S. R., Elsdon, T. S., & Mccarthy, M. D. (2015). Trophic
717 discrimination of nitrogen stable isotopes in amino acids varies with diet quality
718 in a marine fish. Limnology and Oceanography, 60(3), 1076–1087.
719Meng, W., Feagin, R. A., Innocenti, R. A., Hu, B., He, M., & Li, H. (2020). Invasion
720 and ecological effects of exotic smooth cordgrass Spartina alterniflora in China.
721 Ecological Engineering, 143: 105670.
722Miyatake, T., Moerdijk-Poortvliet, T. C. W., Stal, L. J., & Boschker, H. T. S. (2014).
723 Tracing carbon flow from microphytobenthos to major bacterial groups in an
724 intertidal marine sediment by using an in situ 13C pulse-chase method.
725 Limnology and Oceanography, 59(4), 1275–1287.
726Moore, J. W., & Semmens, B. X. (2008). Incorporating uncertainty and prior
727 information into stable isotope mixing models. Ecology Letters, 11(5), 470–480.
728Moreau, S., Boyd, P. W., & Strutton, P. G. (2020). Remote assessment of the fate of
729 phytoplankton in the Southern Ocean sea-ice zone. Nature Communications,
730 11(1).
731Newsome, S. D., Bentall, G. B., Tinker, M. T., Oftedal, O. T., Ralls, K., Estes, J. A., &
732 Fooel, M. L. (2010). Variation in $\delta^{13}C$ and $\delta^{15}N$ diet-vibrissae trophic
733 discrimination factors in a wild population of California sea otters. Ecological
734 Applications, 20(6), 1744–1752.
735Newsome, S. D., Rio, Martinez del, C., Bearhop, S., & Phillips, D. L. (2007). A Niche
736 for Isotope Ecology. Frontiers in Ecology and the Environment, 5(8), 429–436.
737Oakes, J., Connolly, R. M., & Revill, A. T. (2010). Isotope enrichment in mangrove
738 forests separates microphytobenthos and detritus as carbon sources for animals.
739 Limnology and Oceanography, 55(1), 393–402.
740Palmer, M., & Ruhi, A. (2019). Linkages between flow regime, biota, and ecosystem
741 processes: Implications for river restoration. Science, 365(6459).
742Parnell, A. C., Inger, R., Bearhop, S., & Jackson, A. L. (2010). Source partitioning
743 using stable isotopes: Coping with too much variation. PLoS ONE, 5(3).

744Phillips, D. L. (2012). Converting isotope values to diet composition: the use of
745 mixing models. Journal of Mammalogy, 93(2), 342–352.
746Plass-Johnson, J. G., McQuaid, C. D., & Hill, J. M. (2013). Stable isotope analysis
747 indicates a lack of inter- and intra-specific dietary redundancy among
748 ecologically important coral reef fishes. Coral Reefs, 32(2), 429–440.
749Post, D. M. (2002). Using stable isotopes to estimate trophic position: models,
750 methods, and assumptions. Ecology, 83(3), 703–718.
751Qu, P., Zhang, Z., Pang, M., Li, Z., Zhao, L., Zhou, X., … Li, X. (2019). Stable
752 isotope analysis of food sources sustaining the subtidal food web of the Yellow
753 River Estuary. Ecological Indicators, 101, 303–312.
754Ramshaw, B. C., Pakhomov, E. A., Markel, R. W., & Kaehler, S. (2017). Quantifying
755 spatial and temporal variations in phytoplankton and kelp isotopic signatures to
756 estimate the distribution of kelp-derived detritus off the west coast of Vancouver
757 Island, Canada. Limnology and Oceanography, 62(5), 2133–2153.
758Schartup, A. T., Colin, P., Qureshi, A., Dassuncao, C., Gillespie, K., Hanke, A., &
759 Sunderland, E. M. (2019). Climate change and overfishing increase
760 neurotoxicant in marine predators. Nature, 648–650.
761Schmidt, K., Atkinson, a., Stubing, D., McClelland, J. W., Montoya, J. P., & Voss, M.
762 (2003). Trophic relationships among Southern Ocean copepods and krill: some
763 uses and limitations of a stable isotope approach. Limnology and Oceanography,
764 48(1), 277–289.
765Selleslagh, J., Blanchet, H., Bachelet, G., & Lobry, J. (2015). Feeding Habitats,
766 Connectivity and Origin of Organic Matter Supporting Fish Populations in an
767 Estuary with a Reduced Intertidal Area Assessed by Stable Isotope Analysis.
768 Estuaries and Coasts, 38(5), 1431–1447.
769Smit, A. J., Brearley, A., Hyndes, G. A., Lavery, P. S., & Walker, D. I. (2005). Carbon
770 and nitrogen stable isotope analysis of an *Amphibolis griffithii* seagrass bed.
771 Estuarine, Coastal and Shelf Science, 65, 545–556.
772Stasko, A. D., Bluhm, B. A., Michel, C., Archambault, P., Majewski, A., Reist, J. D.,
773 … Power, M. (2018). Benthic-pelagic trophic coupling in an Arctic marine food
774 web along vertical water mass and organic matter gradients. Marine Ecology
775 Progress Series, 594, 1–19.
776Sujitha, S. B., Jonathan, M. P., Aurioles-Gamboa, D., Campos Villegas, L. E.,
777 Bohórquez-Herrera, J., & Hernández-Camacho, C. J. (2019). Trace elements in
778 marine organisms of Magdalena Bay, Pacific Coast of Mexico: Bioaccumulation

779 in a pristine environment. Environmental Geochemistry and Health, 41(3), 1075–
780 1089.
781Tao, W., Niu, L., Liu, F., Cai, H., Ou, S., Zeng, D., … Yang, Q. (2020). Influence of
782 river-tide dynamics on phytoplankton variability and their ecological
783 implications in two Chinese tropical estuaries. Ecological Indicators, 115(4),
784 106458.
785Teichberg, M., Fox, S. E., Olsen, Y. S., Valiela, I., Martinetto, P., Iribarne, O., …
786 Tagliapietra, D. (2010). Eutrophication and macroalgal blooms in temperate and
787 tropical coastal waters: Nutrient enrichment experiments with Ulva spp. Global
788 Change Biology, 16(9), 2624–2637.
789Zhang, M., Huang, G., Liu, C., Zhang, Y., Chen, Z., & Wang, J. (2020). Distributions
790 and origins of nitrate, nitrite, and ammonium in various aquifers in an urbanized
791 coastal area, south China. Journal of Hydrology, 582, 124528.
792Underwood, G. J. C. (2010). Microphytobenthos and phytoplankton in the Severn
793 estuary, UK: Present situation and possible consequences of a tidal energy
794 barrage. Marine Pollution Bulletin, 61(1–3), 83–91.
795Wai, T. C., Leung, K. M. Y., Sin, S. Y. T., Cornish, A., Dudgeon, D., & Williams, G.
796 A. (2011). Spatial, seasonal, and ontogenetic variations in the significance of
797 detrital pathways and terrestrial carbon for a benthic shark, *Chiloscyllium*
798 *plagiosum* (*Hemiscylliidae*), in a tropical estuary. Limnology and Oceanography,
799 56(3), 1035–1053.
800Wai, T.C., Yeung, J. W. Y., Lam, V. Y. Y., Leung, K. M. Y., Dudgeon, D., & Williams,
801 G. A. (2012). Monsoons and habitat influence trophic pathways and the
802 importance of terrestrial-marine linkages for estuary sharks. Ecosphere, 3(1).
803Wang, C., Lv, Y., & Li, Y. (2018). Riverine input of organic carbon and nitrogen in
804 water-sediment system from the Yellow River estuary reach to the coastal zone
805 of Bohai Sea, China. Continental Shelf Research, 157(February), 1–9.
806Wang, Y., Liu, D., Lee, K., Dong, Z., Di, B., Wang, Y., & Zhang, J. (2017). Impact of
807 Water-Sediment Regulation Scheme on seasonal and spatial variations of
808 biogeochemical factors in the Yellow River estuary. Estuarine, Coastal and Shelf
809 Science, 198, 92–105.
810Warne, R. W., Pershall, A. D., & Wolf, B. O. (2010). Linking precipitation and C_3-C_4
811 plant production to resource dynamics in higher-trophic-level consumers.
812 Ecology, 91(6), 1628–1638.

Xu, B., Burnett, W., Dimova, N., Diao, S., Mi, T., Jiang, X., & Yu, Z. (2013). Hydrodynamics in the Yellow River Estuary via radium isotopes: Ecological perspectives. Continental Shelf Research, 66, 19–28.

Yen, J. D. L., Cabral, R. B., Cantor, M., Hatton, I., Kortsch, S., Patricio, J., & Yamamichi, M. (2016). Linking structure and function in food webs: Maximization of different ecological functions generates distinct food web structures. Journal of Animal Ecology, 85(2), 537–547.